Evolution of Long Planetary Wave Packets in a Continuously Stratified Ocean

HUIJUN YANG

Department of Marine Science, University of South Florida, St. Petersburg, Florida

(Manuscript received 19 January 1999, in final form 14 October 1999)

ABSTRACT

Recent TOPEX/Poseidon observations show an enhanced (weakened) westward propagation of long planetary Rossby waves at extratropics (Tropics) and they usually propagate faster in the western basin than in the eastern basin in all major oceans. The evolution of a long planetary wave packet in a continuously stratified ocean in response to the various forcing functions is analytically investigated using the wave packet theory. For a wave packet with a large vertical scale, the stratification variation and the vertical shear of the mean zonal current act in concert, causing the wave packet to propagate directly against the mean zonal current—called the counter-Doppler-shift (CDS) effect. It is found that the speed ratio between the zonal baroclinic zonal current and the classic theory increases with the latitude, the eastward zonal current, and the local vertical scale.

The vertical scale of a wave packet plays a critical role in the propagation, the structure, and spatial-scale development of a wave packet. It is found that the β and stratification effects increase (decrease) the vertical spatial scale of a vertically westward (eastward) tilted wave packet. For a wave packet with a large (small) vertical scale, the vertical spatial scale increases (decreases) when the wave packet is tilted westward in an eastward zonal current. The structural change could effectively separate the extratropic oceanic responses into two kinds of systems with two different vertical scales and strengthen the CDS effect, enhancing speeds in western ocean basins. Several analytical solutions for the wave packet are also obtained.

The author concludes that the evolution of a wave packet with a large vertical scale in a zonal current may account for all major features of the sea surface height anomalies observed in the TOPEX/Poseidon data. The possible forcing functions are the atmospheric wind forcing at the sea surface and the ocean topographic forcing on the seafloor, but not the surface cooling or heating.

1. Introduction

Long planetary Rossby waves play a fundamental role in large-scale ocean dynamics and long-term (years to decades) ocean climate. Using satellite altimetry, only recently have we been able to globally monitor these waves. Data from satellite altimeters are shaping our understanding of long planetary waves and their roles in long-term ocean climate. Using satellite altimetric data from the first three years of the TOPEX/Poseidon mission, Chelton and Schlax (1996) recently conducted the first thorough investigation of long waves in the global ocean. The main features of the observed sea surface height (SSH) anomalies from the TOPEX/Poseidon data are

1) The SSH anomalies with wavelengths larger than 500 km propagate mainly westward at C_r only in the tropical band from 10°S to 10°N, where C_r is the zonal speed of a classic linear free baroclinic long Rossby wave. However, a careful inspection of their results shows that in the tropical band the speed is slightly less than the theoretical one C_r for the Atlantic and Indian Ocean estimates.
2) Poleward of this band, the ratio of the observed phase speed to the theoretical one tend to increase monotonically from 1 to more than 2 in the Northern Hemisphere and 1 to more than 3 in the Southern Hemisphere. In the Antarctic Circumpolar Current this ratio is as high as four.
3) These waves propagate faster in the western basin than in the eastern basin (also G. Mitchum 1998, personal communication).

The westward propagating baroclinic Rossby waves have been observed in many studies (e.g., White 1977, 1985; Kang and Magaard 1980; Kessler 1990; Jacobs et al. 1993, 1994; Polito and Cornillon 1997; among many others). The theory for long Rossby waves is well known (Phillips 1965; Platzman 1968; Dickinson 1978; Gill 1982) and holds for an ocean whose background state is at rest. The zonal phase speeds of baroclinic modes decrease with latitude and may be a few centimeters per second. Thus these waves take only a few months to cross an ocean basin in the Tropics, but years to decades at higher latitudes.

Corresponding author address: Dr. Huijun Yang, Department of Marine Science, University of South Florida, 140 Seventh Avenue South, St. Petersburg, FL 33701-5016.
E-mail: yang@marine.usf.edu

Several mechanisms have been proposed in the past that may help to explain the high zonal phase speeds of these observed long planetary Rossby waves. First, White (1977) suggested that under direct surface wind forcing, the ocean response that consisted of a directly forced wave and a free, baroclinic Rossby wave could propagate westward at $2C_r$.

Killworth et al. (1997) showed that inclusion of the mean zonal current works to increase the westward propagation of free, baroclinic Rossby waves by changing the meridional gradient of the background potential vorticity. Dewar (1998) recently used a three-layer model and argued that baroclinic waves in a shear flow are accelerated to the west via their interactions with both the mean advective field and the mean potential vorticity field.

However, we know little about the vertical structures of these long planetary Rossby waves, how these waves change their structures in the mean ocean circulation, and whether these changes may be manifested in the observed TOPEX/Poseidon data. The purposes of this paper are to account for all major features of the observed zonal wave speeds of the long planetary Rossby waves and to investigate how the structures of these waves may change in time and whether these changes may help us better understand the TOPEX/Poseidon observations. Instead of using a normal mode method as in Killworth et al. (1997) or a layered-model as in Dewar (1998), in this paper we employ a continuously stratified model and the wave packet approximation. We consider the evolution of a long planetary wave packet in the zonal current in response to various forcing functions. It is found that the stratification variation and the vertical shear of the mean zonal current acts in concert and causes the wave packet to propagate directly against the mean ocean circulation. We call this the counter-Doppler-shift effect. Our results not only highlight the importance of the mean zonal current on wave propagation, as in Killworth et al. (1997) and Dewar (1998), but also the critical role the vertical scale of a wave packet plays in the wave packet development. We conclude that it is the atmospheric wind forcing at the sea surface and the ocean topographic forcing on the sea floor, not the surface cooling or heating, that may be responsible for these long planetary waves. The evolution of a long planetary wave packet in the zonal current in response to these forcing functions may account for all major features observed in the TOPEX/Poseidon data.

The wave packet approximation is one form of the WKB approximation. This or a similar approach has been widely used in the atmospheric and oceanic studies. One of advantages over conventional methods is that this approach allows one to investigate not only the propagation properties of a wave system, but also its structural changes. Yang (1991) traced its history and systematically presented the theory. The reader is referred to the monograph for a general discussion on the theory and its applications in geophysical fluid dynamics.

We start with the mathematical formulations in the next section, followed by a discussion on the counter-Doppler-shift (CDS) effect, which is critical for explaining the observed wave propagation features in section 3. In section 4, we study the structures and structural changes of the wave packet with some complete analytic solution of the wave packet evolution. We discuss our results in section 5, followed by major conclusions in last section.

2. Mathematical formulations

a. Linearized potential vorticity equation

The linearized nondimensional equation governing the potential vorticity in a stratified three-dimensional quasigeostrophic baroclinic ocean for large-scale motion can be written as

$$\left(\frac{\partial}{\partial t} + U(z)\frac{\partial}{\partial x}\right)q' + B\frac{\partial \psi'}{\partial x} = 0, \tag{2.1}$$

where q' is the perturbation potential vorticity, defined by

$$q' = \frac{\partial^2 \psi'}{\partial x^2} + \frac{\partial^2 \psi'}{\partial y^2} + \frac{\partial}{\partial z}\left(\frac{1}{S}\frac{\partial \psi'}{\partial z}\right); \tag{2.2}$$

B is the meridional gradient of the mean potential vorticity (Q), defined by

$$B = \frac{\partial Q}{\partial y} = \beta - \frac{\partial}{\partial z}\left(\frac{1}{S}\frac{\partial U}{\partial z}\right); \tag{2.3}$$

and S is the nondimensional stratification parameter, defined by

$$S = \frac{N^2 D^2}{L^2 f_0^2}. \tag{2.4}$$

Here N is the Brunt–Väisälä frequency; L and D are the horizontal and vertical characteristic scales, respectively; f_0 is the Coriolis parameter; β is the meridional gradient of the Coriolis parameter; $U(z)$ is the mean zonal ocean current; and x, y, and z are eastward, northward, and upward coordinates. One can easily obtain this equation from standard stratified geophysical fluid dynamics in mean baroclinic currents (Pedlosky 1987; Yang 1991).

b. Vertical profiles of the basic state

We assume that the stratification parameter is an exponential function of z with a scale H; namely

$$S = S_0 e^{z/H}, \tag{2.5}$$

where S_0 is the value of the stratification parameter at $z = 0$. Exponential stratification is rather realistic for

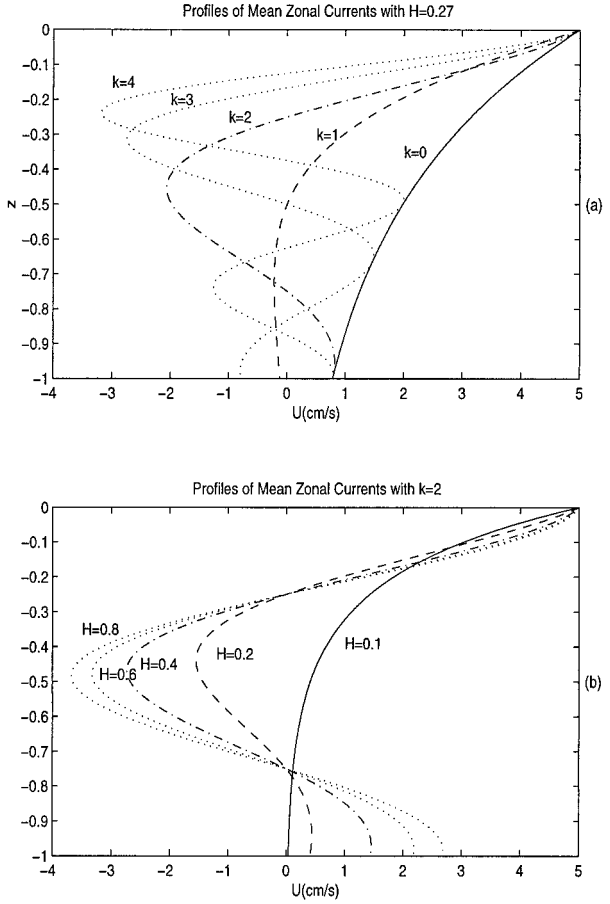

FIG. 1. Vertical profiles of mean zonal currents (a) for different vertical modes with $H = 0.27$ and (b) for different exponential scale H with $k = 2$, $U_s = 5$.

the global subsurface ocean and has been widely used (e.g., Gill et al. 1974; Pedlosky 1987). For example, based on a realistic fit to the Levitus and Bobyer (1994) and Levitus et al. (1994) North Atlantic data, N^2 can be fitted into this function with $H = 1/3.7 = 0.27$, according to Killworth et al. (1997).

Next we assume that the mean zonal ocean circulation takes the following general form:

$$U = U_s e^{z/2H}/\cos(k\pi z), \tag{2.6}$$

where k is the vertical mode number of the mean zonal ocean current and U_s is the zonal mean current at the sea surface (or in the upper thermocline). There are two reasons for taking this mean zonal current. First it greatly simplifies the problem, and second this form is more reasonable than the pure normal mode. Figure 1 shows profiles of mean zonal currents for different vertical modes (Fig. 1a) and different exponential scales H (Fig. 1b). It shows that the counter-undercurrent becomes strong and its jet center moves upward as the vertical mode increases. This form captures not only the decaying characteristics of the mean zonal current, but also accurately describes its slower-than-stratification decaying rate with ocean depth (Gill et al. 1974; Killworth et al. 1997).

A net zonal transport by this mean circulation is

$$\overline{U} = U_s \frac{4H^2}{1 + 4H^2k^2\pi^2}\left[1 - \frac{(-1)^k}{e^{1/(2H)}}\right]. \tag{2.7}$$

The character of these vertical profiles of the stratification and mean ocean circulation is more realistic than in most layer models and its realism has long been recognized (Gill et al. 1974; Killworth et al. 1997). However, due to its mathematical difficulty these kinds of vertical profiles are rarely used in ocean dynamics analysis.

With these stratification and mean zonal current distributions, the potential vorticity gradient becomes

$$B = \beta + \frac{U}{4H^2S} + \frac{k^2\pi^2U}{S}. \tag{2.8}$$

The first term on the right-hand side represents the beta effect, which is always positive. The second term represents the effect of exponential variation in the basic state. This effect increases the mean potential vorticity gradient in the eastward mean circulation and decreases the gradient in the westward mean circulation. The last term represents the effect of the vertical mode of the mean zonal circulation. Thus, the gradient of mean potential vorticity increases in the eastward mean circulation and decreases in the westward mean circulation. This can be understood as follows. In an eastward mean baroclinic zonal circulation the thermocline depth has to increase with latitude, while in a westward mean baroclinic zonal circulation, the thermocline depth has to decrease with latitude. As a result, the mean baroclinic zonal current acts like slope topography. The sloping topography induces the change in the gradient of the mean potential vorticity.

By use of the transformation

$$\psi' = e^{z/2H}\psi, \tag{2.9}$$

we can write the perturbation Eq. (2.1) in the following form:

$$\left(\frac{\partial}{\partial t} + U(z)\frac{\partial}{\partial x}\right)q + B\frac{\partial\psi}{\partial x} = 0, \tag{2.10}$$

where

$$q = -\frac{\psi}{4H^2S} + \frac{\partial^2\psi}{\partial x^2} + \frac{1}{S}\frac{\partial^2\psi}{\partial z^2}, \tag{2.11}$$

$$B = \beta + \frac{1 + 4H^2k^2\pi^2}{4H^2S}U, \tag{2.12}$$

and for simplicity the perturbation has been assumed independent of y for long planetary waves.

c. Equations governing the wave packet evolution

We simplify an individual single oceanic disturbance system as a wave packet that may consist of several waves and vary with space and time. The forcing functions for the oceanic disturbance system could be the atmospheric wind stress at the sea surface or sea surface cooling or heating. The ocean topography of the sea floor is another potential source for the oceanic disturbance. However, we do not need to specify the forcing function here since we could treat the disturbance system as a free system after being initiated by these forcing functions.

The sea surface height anomalies observed in the TOPEX/Poseidon data have a large horizontal scale of several hundred kilometers, but still much smaller than the ocean basin scale of several thousand kilometers. However, the TOPEX/Poseidon observations cannot provide any information on the vertical scale of the perturbation, which is responsible for these anomalies. We may assume that the disturbance system mainly is concentrated within the thermocline whose vertical scale is much smaller than the ocean depth. We thus suppose that the mean zonal ocean current U, the stratification parameter S, and the mean potential vorticity gradient B in (2.7) are slowly varying with respect to space.

Following Yang (1987, 1991), we introduce the slowly varying variables

$$T = \epsilon t, \qquad X = \epsilon x, \qquad Z = \epsilon z, \tag{2.13}$$

and

$$\psi = \Psi(X, Z, T)e^{i\theta(X, Z, T)/\epsilon}, \tag{2.14}$$

where

$$\Psi = \Psi_0(X, Z, T) + \epsilon\Psi_1(X, Z, T) + \epsilon^2\Psi_2(X, Z, T) + \cdots. \tag{2.15}$$

Here ϵ is a small nondimensional parameter, which is ratio between the horizontal scale of the wave packet and that of an ocean basin.

Define

$$\sigma = -\frac{\partial\theta}{\partial T}, \qquad m = \frac{\partial\theta}{\partial X}, \qquad l = \frac{\partial\theta}{\partial Z} \tag{2.16}$$

as local frequency and local wavenumbers in the x and z direction, respectively. We then have the following relations:

$$\frac{\partial\sigma}{\partial X} = -\frac{\partial m}{\partial T}, \qquad \frac{\partial\sigma}{\partial Z} = -\frac{\partial l}{\partial T}, \quad \text{and} \tag{2.17}$$

$$\frac{\partial m}{\partial Z} = \frac{\partial l}{\partial X}. \tag{2.18}$$

Substituting these definitions and relations into the governing equation, we obtain, at the lowest order, the dispersion relationship

$$\sigma = Um - \frac{m}{K^2}B, \tag{2.19}$$

where

$$K^2 = m^2 + \frac{l^2}{S} + \frac{1}{4H^2S}. \tag{2.20}$$

At the next higher order, we have the amplitude equation as follows:

$$\left(\frac{\partial}{\partial T} + U\frac{\partial}{\partial X}\right)(K^2\Psi_0) - B\frac{\partial\Psi_0}{\partial X} + \frac{mB}{K^2}\left[2\left(m\frac{\partial}{\partial X} + l\frac{\partial}{\partial Z}\right)\Psi_0 + \Psi_0\left(\frac{\partial m}{\partial X} + \frac{\partial l}{\partial Z}\right)\right] = 0. \tag{2.21}$$

From the dispersion relation (2.19), we have the wave phase velocity in x and z, respectively,

$$C_X = U - \frac{B}{K^2} \tag{2.22}$$

$$C_Z = U\frac{m}{l} - \frac{m}{lK^2}B \tag{2.23}$$

and two components of the group velocity in the X and Z direction, respectively,

$$C_{gX} = \frac{\partial\sigma}{\partial m} = U - \frac{K^2 - 2m^2}{K^4}B \tag{2.24}$$

$$C_{gZ} = \frac{\partial\sigma}{\partial l} = \frac{2ml}{SK^4}B. \tag{2.25}$$

Using (2.16), the definitions of σ, m, and l, (2.19), the dispersion relationship, and the above group velocity yields

$$\frac{D_g\sigma}{DT} = 0 \tag{2.26}$$

$$\frac{D_g m}{DT} = 0 \tag{2.27}$$

$$\frac{D_g l}{DT} = -\left(m\frac{\partial U}{\partial Z} - \frac{(1 + 4H^2l^2)m}{4H^3SK^4\epsilon}B - \frac{m}{K^2}\frac{\partial B}{\partial Z}\right), \tag{2.28}$$

where the operator D_g/DT is defined by

$$\frac{D_g}{DT} = \frac{\partial}{\partial T} + C_{gX}\frac{\partial}{\partial X} + C_{gZ}\frac{\partial}{\partial Z}. \tag{2.29}$$

Therefore, we have obtained all the equations governing the evolution of the planetary wave packet. Equations (2.24)–(2.25) describe the wave packet propagation, whereas Eqs. (2.27)–(2.28) are for the structural change of the wave packet. Equation (2.26) shows that the local frequency does not change with time along the wave packet pathway because the mean state is steady.

Let

$$\Psi_0 = |\Psi_0(X, Z, T)|e^{i\alpha/(X, Z, T)}, \tag{2.30}$$

where $|\Psi_0|$ is the real amplitude and α is the phase of the wave packet. Substituting (2.30) into the amplitude Eq. (2.21) and separating the real and imaginary parts, we have

$$\frac{D_g\alpha}{DT} = 0, \tag{2.31}$$

$$\left(\frac{\partial}{\partial T} + U\frac{\partial}{\partial X}\right)(K^2|\Psi_0|) - B\frac{\partial|\Psi_0|}{\partial X} - \frac{mB}{K^2}\left[2\left(m\frac{\partial}{\partial X} + l\frac{\partial}{\partial Z}\right)|\Psi_0| + |\Psi_0|\left(\frac{\partial m}{\partial X} + \frac{\partial l}{\partial Z}\right)\right] = 0. \tag{2.32}$$

Equation (2.31) demonstrates that the energy of the wave packet propagates with group velocity, whereas Eq. (2.32) describes the evolution of the real amplitude of the wave packet.

d. Long planetary wave approximation

For long planetary Rossby waves, we can simplify the formulation further. The stratification parameter S can also be written as

$$S = \left(\frac{L_D}{L}\right)^2, \tag{2.33}$$

where

$$L_D = \sqrt{\frac{N^2D^2}{f_0^2}}$$

is the Rossby deformation radius. For the very long planetary waves that have been observed by satellite altimetry, L is much larger than L_D. Thus, S is less than unity and Eq. (2.20) becomes

$$K_l^2 = K^2 = \frac{l^2}{S} + \frac{1}{4H^2S} = \frac{1 + 4H^2l^2}{4H^2S}. \tag{2.34}$$

As the result, the long planetary wave packet group velocity becomes

$$C_{gX} = U - \frac{S}{l^2 + 1/(4H^2)}B, \tag{2.35}$$

$$C_{gZ} = \frac{2mlS}{[l^2 + 1/(4H^2)]^2}B. \tag{2.36}$$

In this case, the zonal component of the group velocity (2.35) is the same as the zonal phase velocity (2.22).

The equations governing the structural change of the long planetary wave packet become

$$\frac{D_gm}{DT} = 0. \tag{2.37}$$

$$\frac{D_gl}{DT} = -\left(m\frac{\partial U}{\partial Z} - \frac{4HSm}{\epsilon(1 + 4H^2l^2)}B - \frac{4H^2Sm}{1 + 4H^2l^2}\frac{\partial B}{\partial Z}\right). \tag{2.38}$$

We will only consider these long planetary wave packets in this study.

3. The counter-Doppler-shift effect

a. Zonal propagation speed

The zonal speed of the planetary wave packet (2.35) can be written as

$$C_X = C_{gX} = U - \frac{4H^2S}{1 + 4H^2l^2}B \quad \text{or} \tag{3.1}$$

$$C_X = C_{gX} = U - \frac{4H^2S}{1 + 4H^2l^2}\beta - \frac{1 + 4H^2k^2}{1 + 4H^2l^2}U. \tag{3.2}$$

The first term represents advection of the mean zonal current effect, namely the Doppler-shift effect. The second term is the classic beta effect, resulting in the westward propagation of long planetary waves. The third term represents the effects of stratification variation and the shear of the mean zonal circulation.

The zonal speed can be rewritten as

$$C_X = C_{gX} = -\frac{4H^2S}{1 + 4H^2l^2}\beta + \left[1 - \frac{1 + 4H^2k^2\pi^2}{1 + 4H^2l^2}\right]U. \tag{3.3}$$

b. Non Doppler shift

If the vertical mode of the long planetary Rossby wave packet is the same as the vertical mode of the mean zonal circulation (i.e., $l = k\pi$), we have

$$C_X = C_{gX} = C_r = -\frac{4H^2S\beta}{1 + 4H^2k^2\pi^2}. \tag{3.4}$$

Thus, the Doppler shift by the advection of the mean circulation exactly cancels the effect of the exponential variation of the basic state. This produces the non-Doppler-shift phenomenon, which has been observed for long planetary waves in the 1½-layer model and noted by other investigators, mentioned in the introduction.

c. Counter Doppler shift

If the vertical scale of the wave packet is larger than that of the stratification scale H, that is, $1/l^2 \gg 4H^2$, we have

$$C_X = C_{gX} = -4H^2S\beta - 4H^2k^2\pi^2U. \tag{3.5}$$

In this case, the presence of the mean zonal current

causes the wave packet to propagate directly against the background current; we call it the counter-Doppler-shift effect. This effect has been noted recently by Dewar (1998). The CDS will enhance the westward propagation of a wave packet in an eastward zonal current and slow down the westward propagation in a westward zonal current.

d. Advection effect

If the vertical scale of a wave packet is much smaller than that of the vertical mode of the mean zonal current, that is, $l^2 \gg k^2\pi^2 > 1$, then we have

$$C_X = C_{gX} = -\frac{S}{l^2}\beta + U. \tag{3.6}$$

The mean zonal current directly forces the wave packet to propagate along the mean current if one can neglect the beta effect since l^2 is large and S is small.

e. Speed ratios

We can easily calculate the zonal wave speed ratio between the speed given by (3.3) and classic speed C_r, at the sea surface,

$$R = \frac{C_X}{C_r} = 1 + \frac{k^2\pi^2 - l^2}{S_0\beta}U_s. \tag{3.7}$$

The nondimensional variables and parameters are related to the dimensional variables by $\beta = \beta_0 L^2/U_0$, where U_0 is the zonal velocity scale and β_0 is the derivative of the Coriolis parameter, and $U_s^* = U_0 U_s$, where U_s^* is the dimensional surface zonal current. The zonal speed ratio becomes

$$R = 1 + \frac{f_0^2 U_s^*}{N_s^2 D^2 \beta_0}(\pi^2 k^2 - l^2), \tag{3.8}$$

where (2.4) has been used. Thus, this ratio increases with latitude, the strength of the eastward zonal current, the vertical mode number of the zonal mean current, and the vertical scale of the wave and decreases with the buoyancy frequency and the ocean depth in an eastward mean circulation.

In the higher latitudes of the subtropical gyre, the mean zonal circulation is eastward and thus these ratios are greater than one. In the lower latitudes, the mean zonal circulation is westward and thus these ratios are less than one, as also noted by Dewar (1998). Since in the extratropic western basin, the eastern current is stronger than that in the eastern basin. The results show that the speeds are higher in the western basin than in the eastern basin. These are all consistent with the TOPEX/Poseidon observations (to be discussed further in last section).

For the global oceans at the midlatitudes, we take the following realistic values $f_0 = 10^{-4}$ s^{-1}, $N_s^2 = 40 \times 10^{-6}$ rad^2 s^{-2}, $\beta_0 = 2.3 \times 10^{-13}$ s^{-1} cm^{-1}, $U_s^* = 5$ cm s^{-1} and $D = 4.5$ km. Figure 2 shows the zonal speed ratio variations with the latitude for various surface mean zonal currents (a) and for various vertical modes of the mean zonal current (b). The effect of a change in the buoyancy frequency on the ratio can be viewed as the change in the surface zonal current as shown Fig. 2a. The results show that these ratios are greater than one in higher latitudes. One striking feature of these results is that near the polar region, the ratios can be as high as three or four. This is also consistent with the observed ratios in the Antarctic Circumpolar Current (ACC).

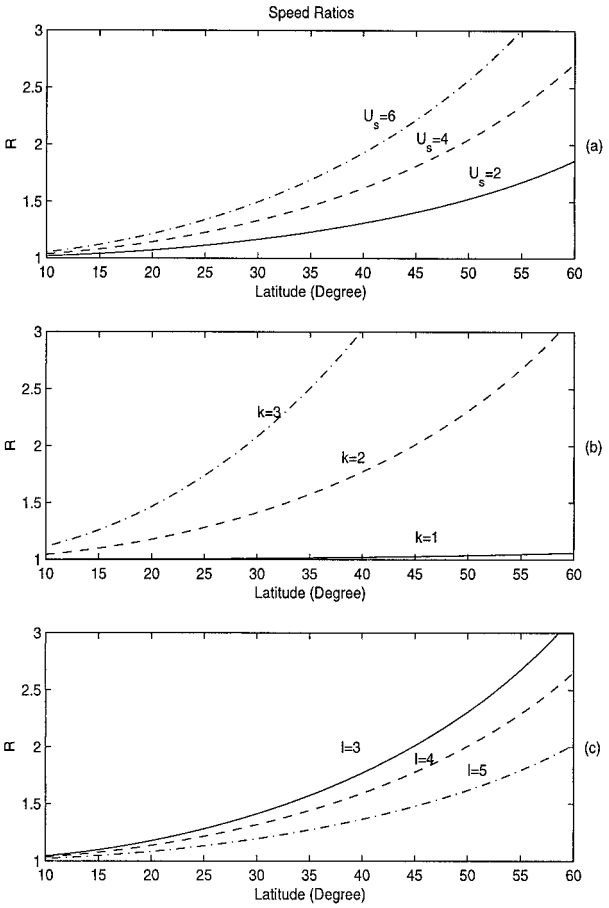

FIG. 2. Zonal speed ratios between this theory and the classic one (a) for various surface currents with $k = 2$, $l = 3$; (b) for various vertical modes with $U_s = 5$ cm s^{-1}, $l = 3$; and (c) for different vertical scale l with $U_s = 5$ cm s^{-1}, $k = 2$. Other parameters are the same as given in the text.

If we extend our model to the lower latitudes and take the following typical parameter values, $l = 3$, $U_s = -10$ cm s^{-1}, $k2$ and $D = 4.5$ km at a latitude of 8° (not shown), we have $R = 0.8$. Therefore, these results are consistent with all observed features of the long planetary Rossby waves described in the introduction.

Even though these results show that the zonal wave speed ratio increases with latitude, the vertical mode 2 may best account for the observed wave speeds in the

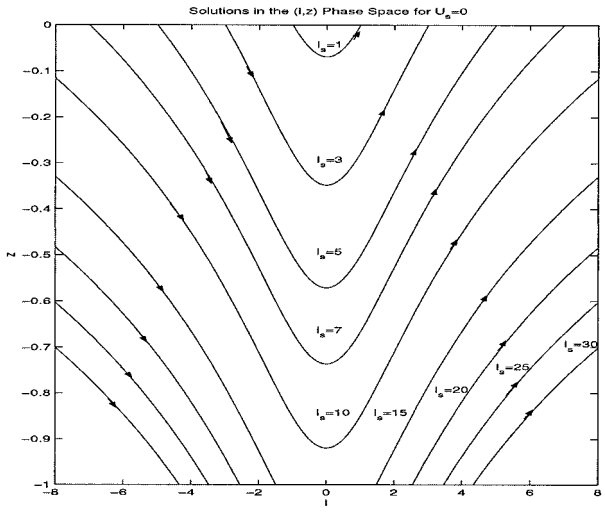

FIG. 3. Wave packet solutions in the (l, z) phase space in the absence of a mean current. The wave packets evolve from the left to right along their pathways. Numbers denote the different l.

extratropics. The importance of mode 2 of the general circulation also has been recognized by Killworth et al. (1997) and Dewar (1998). In the presence of a nonzero wavenumber l, other vertical modes of the mean zonal current may equally well account for the observed wave speed ratios. Figure 2c shows the variation of the wave speed ratio with the local vertical wavenumber l. It is important to recognize that the wave speed ratios are different for different l. The speed ratio decreases with local vertical wavenumber or increases with the local vertical scale. Thus, the vertical structure of the wave packet may greatly affect what we may observe at the sea surface.

4. Structural changes

a. Vertical structures

The group velocities (3.3) and (2.36) read

$$C_{gX} = -\frac{4H^2S}{1 + 4H^2l^2}\beta - 4H^2\frac{k^2\pi^2 - l^2}{1 + 4H^2l^2}U \quad (4.1)$$

$$C_{gZ} = \frac{32H^4Sml}{(1 + 4H^2l^2)^2}B. \quad (4.2)$$

For a wave packet tilted westward with z upward (or eastward with the ocean depth, i.e., the negative z direction), $ml < 0$, whereas for a wave packet tilted eastward with z upward (or westward with the ocean depth), $ml > 0$. We call the former the westward tilted wave packet and the latter the eastward tilted wave packet. Without loss of generality, we assume that m is always positive. Thus, for a westward tilted wave packet, its local vertical wavenumber l is negative, whereas for an eastward tilted wave packet, the wavenumber l is positive.

In eastward zonal currents, a long planetary wave packet propagates toward the west. The zonal speed of the wave packet increases vertically upward with z (or decreases with the ocean depth) because of the decaying of stratification and the mean zonal current with ocean depth. As a result, a wave packet is tilted westward in the extratropics. For a westward tilted wave packet ($ml < 0$), the group velocity in the z direction is negative, that is downward from (4.2). Thus the wave energy as well as the wave packet itself will propagate downward. However, the downward propagation is much slower than the westward propagation because of small m for a long planetary wave packet.

b. Structural changes

Equations that govern the wavenumbers or the spatial scale of the wave packet, (2.37) and (2.38), are

$$\frac{D_g m}{DT} = 0, \quad (4.3)$$

$$\frac{\epsilon D_g l}{DT} = \frac{m}{1 + 4H^2l^2}\{4HS\beta + 2H(k^2\pi^2 - l^2) \times U[1 - 2Hk\pi \tan(k\pi z)]\}. \quad (4.4)$$

The first equation states that the zonal spatial scale of the wave packet will not change with time because the basic state of the ocean is uniform in the zonal direction. The second equation describes the vertical spatial scale change with time. We can easily rewrite the equation in the following form:

$$\frac{\epsilon}{2}\frac{D_g l^2}{DT} = \frac{ml}{1 + 4H^2l^2}\{4HS\beta + 2H(k^2\pi^2 - l^2) \times U[1 - 2Hk\pi \tan(k\pi z)]\}. \quad (4.5)$$

1) THE β EFFECT

In the absence of a mean zonal current, we have

$$\frac{\epsilon D_g l^2}{DT} = \frac{4HS\beta ml}{1 + 4H^2l^2}. \quad (4.6)$$

Thus, the vertical local wavenumber increases with β and S. The westward-tilted wave packet will increase its vertical spatial scale and decrease its westward tilt. For an eastward-tilted wave packet, the vertical spatial scale will decrease and increase its eastward tilt.

2) LARGE VERTICAL SCALE

When the vertical scale of a wave packet is large compared to the vertical mode scale of the mean current, $l^2 < k^2\pi^2$, we have

$$\frac{\epsilon}{2}\frac{D_g l^2}{DT} = \frac{2Hk^2\pi^2 Uml}{1 + 4H^2l^2}\{[1 - 2Hk\pi \tan(k\pi z)]\}. \quad (4.7)$$

In the eastward current, the local vertical wavenumber increases (decreases) in an eastward mean current when the wave packet is tilted eastward (westward). In a westward mean current, the wavenumber decreases (increases) with time when the packet is tilted eastward (westward). Accordingly, the vertical spatial scale of the wave packet decreases (increases) in an eastward mean current for an eastward (westward) tilted packet. The vertical scale increases (decreases) in a westward mean current for an eastward (westward) tilted packet.

3) Small vertical scale

For a wave packet with a vertical scale smaller than that of the vertical mode of the mean current, $l^2 > k^2\pi^2$, we have

$$\frac{\epsilon}{2}\frac{D_g l^2}{DT} = -\frac{2HUml^3}{1 + 4H^2l^2}\{[1 - 2Hk\pi \tan(k\pi z)]\}. \quad (4.8)$$

In the eastward current, the vertical spatial scale of the wave packet decreases (increases) in the eastward mean current for an eastward (westward) tilted packet. The vertical scale increases (decreases) in the westward mean current for an eastward (westward) tilted packet.

It is interesting to note that for an eastward current, a westward tilted wave packet with a large (small) vertical scale will enlarge (shrink) its vertical scale. This may result in two different kinds of wave packets with different vertical scales.

c. Analytic solution

Using a characteristic method (Courant and Hilbert 1962), we can write the partial differential equations governing the local wavenumbers and wave packet path as a system of ordinary differential equations as follows:

$$\frac{dm}{dT} = 0, \quad (4.9)$$

$$\frac{\epsilon dl}{dT} = \frac{m}{(1 + 4H^2l)}\{4HS\beta + 2H(k^2\pi^2 - l^2) \times U[1 - 2Hk\pi \tan(k\pi z)]\} \quad (4.10)$$

$$\frac{dX}{dT} = C_{gX} = -\frac{4H^2S}{1 + 4H^2l^2}\beta - 4H^2\frac{k^2\pi^2 - l^2}{1 + 4H^2l^2}U \quad (4.11)$$

$$\frac{dZ}{dT} = C_{gZ} = \frac{32H^4Sml}{(1 + 4H^2l^2)^2}B. \quad (4.12)$$

The characteristics of the wave packet are exactly the pathways of the packet determined by the group velocity.

In the absence of a mean zonal current, $U_s = 0$, the equations that govern the evolution of a long planetary wave packet become

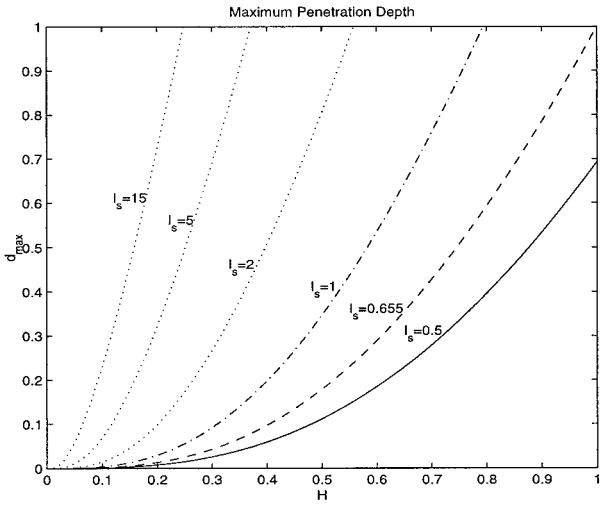

FIG. 4. Variation of the maximum penetration depth of the wave packet in the medium at rest with H.

$$\frac{dm}{dT} = 0 \quad (4.13)$$

$$\frac{\epsilon dl}{dT} = \frac{4HSm}{1 + 4H^2l^2}\beta \quad (4.14)$$

$$\frac{dX}{dT} = -\frac{4H^2S}{1 + 4H^2l^2}\beta \quad (4.15)$$

$$\frac{dZ}{dT} = \frac{32H^4Sml}{(1 + 4H^2l^2)^2}\beta. \quad (4.16)$$

Since the second equation only depends on Z, we can easily solve the equation and use (4.12) to obtain the analytical solution for l, z:

$$1 + 4H^2l^2 = (1 + 4H^2l_s^2)e^{z/H}, \quad (4.17)$$

where l_s is the wavenumber at the sea surface, $z = 0$. Figure 3 shows the flow diagram for the evolution of long planetary wave packets without a mean zonal current in the (l, z) phase space. The wave packet evolution follows from negative l to positive l as time increases. When a wave packet is tilted westward (l is negative), it propagates downward. When a wave packet is tilted eastward (l is positive), it propagates upward. For a given wave packet with wavenumber, l_s, the deepest ocean depth it can reach is determined by

$$d_{\max} = H \ln(1 + 4H^2l_s^2). \quad (4.18)$$

This depth increases with increasing l_s. Thus only the wave packet with a vertical wavenumber at the sea surface l_s larger than $L_s = \sqrt{(e^{1/H} - 1)}/(2H)$, can reach the ocean bottom. Figure 4 illustrates the variation of the maximum penetration depth of the wave packet with H for different local wave numbers.

We can obtain the complete solution:

$$m = m_s \tag{4.19}$$

$$l = -\frac{4H^2S_0m\beta}{1 + 4H^2l_s^2}(t_s - t) - |l_s| \tag{4.20}$$

$$X = X_s + \frac{4H^2S_0\beta}{1 + 4H^2l_s^2}(t_s - t) \tag{4.21}$$

$$z = H \ln\{(1 + 4H^2l_s^2)^2 + [8H^2S_0m\beta(t_s - t) + 2Hl_s(1 + 4H^2l_s^2)]^2\} - 3H \ln(1 + 4H^2l_s^2), \tag{4.22}$$

where m_s is the zonal local wavenumber of the wave packet at the sea surface. Other wave packet solutions in different situations are also found and given in the Appendix for future reference.

5. Discussions

a. Relevance to TOPEX/Poseidon observations

These results may help to explain a number of important observed features from the TOPEX/Poseidon data, some of which have not been well explained in the previous studies. First, the speed ratio between observed and the linear theory prediction is not two or a constant, as some previous studies would assume. This speed ratio, in fact, is increased with latitude. This study predicts that this increase is proportional to $\sin(\theta)^2/\cos(\theta)$ with latitude θ, consistent with the observations.

Second the counter-Doppler-shift effect of these planetary wave packets with a large vertical scale is also critical since this effect has the same order magnitude as the beta effect. It is this CDS effect that is responsible for the enhanced potential vorticity gradient and the enhanced wave speed in an eastward current. Assuming other parameters are the same, the westward propagation of the wave packet will be faster in a strong eastward current than in a weak current. Since the current increases westward in the extratropics, this may partially explain why the observed speed ratio is higher in a western basin than in an eastern basin. However, in the Tropics, since the current is westward, the CDS effect will tend to make the wave packet propagate to the east, thus weakening the westward propagation due to the beta effect. In addition, combined with the increase in the speed ratio with latitude as just discussed, in the Antarctic Cir Current, the strong eastward current at high latitudes makes the speed ratios even higher and they can be as high four, as observed (Chelton and Schlax 1996). The current results can easily account for such a high ratio at the ACC.

b. Different regimes and forcing functions

The vertical spatial scale of a wave packet plays a critical role in distinguishing different wave packet regimes from non Doppler shift, counter Doppler shift, to advection. Our results show that for the perturbation with a large vertical scale, it will behave like the non-Doppler-shift mode or counter-Doppler-shift mode whereas for a perturbation with a small vertical scale it will behave like the advection mode.

What generates the perturbations with different vertical scales in the ocean? There are various forcing functions that may be possibly responsible for the long planetary waves observed in the TOPEX/Poseidon data. First, it is well known that a zonal symmetric atmospheric wind forcing at the sea surface will likely generate a barotropic response in the ocean thermocline, thus a relative large vertical-scale ocean perturbation. But a zonal asymmetric wind forcing can generate both barotropic and baroclinic ocean responses, thus large and small vertical-scale perturbations. Second, the surface cooling or heating will likely generate a baroclinic ocean response, giving a relatively small vertical ocean perturbation.

Our theory predicts that the response from the zonal symmetric wind forcing will likely behave like the non-Doppler-shift mode and counter-Doppler-shift mode since they tend to have a large vertical scale. On the other hand, the response from the surface cooling or heating will likely behave like the advection mode. These predictions are consistent with recent two-layer thermocline studies of Huang and Pedlosky (1999) and will hold in the ocean gyre circulation (Yang 2000, manuscript submitted to *J. Phys. Oceanogr.*).

Even though the atmospheric wind forcing at the sea surface will generate both barotropic-like and baroclinic-like responses, the signal in the sea surface height as observed in TOPEX/Poseidon data represents the vertical integral part of the response with a large vertical scale. Thus, the sea surface height anomalies due to atmospheric wind forcing will behave like the non-Doppler-shift mode and counter-Doppler-shift mode, not the advection mode. The advection-like mode, however, does occur in the thermocline temperature or salinity anomalies (Huang and Pedlosky 1999; Liu 1999; Yang 2000). In addition, the structural change of a wave packet will tend to strengthen the response with a large vertical scale as the wave packet propagates into the western basin (see more discussion below).

The third important forcing function for the oceanic disturbance is the topography on the ocean floor, especially the ocean ridges in the mid Atlantic and Pacific. By the same token, the disturbance from the ocean topographic forcing will likely have a relatively large vertical scale and a strong barotropic character and thus behave like the counter-Doppler-shift mode. Not only could the ocean topography act as the source of the disturbance system, but also the slope of the ocean topography may alter the propagation and structure of the perturbations, as discussed in Yang (1987, 1991). Of course, the influence of topography on generating signals is more complex in reality. For instance, barotropic modes may be scattered into baroclinic modes by in-

teracting topography. This, however, is beyond our discussion in this study.

Therefore, it is likely that the atmospheric wind forcing at the sea surface and topographic forcing on the ocean floor are ultimately responsible for those long planetary wave packets whose features were observed in the TOPEX/Poseidon data. Considering strong annual and interannual variability of the atmospheric wind at the sea surface and relatively large midocean ridges, there should be numerous sources for these long planetary wave packets in the world oceans. Strong annual and interannual variability in the atmospheric wind forcing at the sea surface will definitely induce strong ocean responses on these timescales and as well as longer time scales of these long planetary wave packet propagations.

c. Structures and their changes

Even though the TOPEX/Poseidon observations cannot provide any information on the vertical structures and their changes in the ocean perturbation systems, it does not mean that the disturbance system responsible for these observed SSH anomalies does not have a vertical structure, or only has a fixed one. On the contrary, observations show that the thermocline perturbation anomalies do move vertically and change their vertical scales with time (e.g., Fig. 1 of Schneider et al. 1999).

The vertical structures in the extratropical ocean may be likely titled westward with z upward. In general, the current in the upper layer is larger than in the lower layer. A wave packet with a large vertical scale will behave like the counter-Doppler-shift mode. A perturbation system induced by atmospheric wind forcing at the sea surface or by topographic forcing on the ocean floor will propagate westward with different speeds due to the vertical shear of the circulation. The upper part of the wave packet will propagate westward faster than its lower part. As a result, the perturbation will be vertically tilted westward. By the same token, a large vertical-scale perturbation will tilt to the east vertically in the westward current due to the vertical shear in the circulation.

The beta effect and stratification will increase the vertical spatial scale of a westward tilted wave packet. In addition, in the extratropics a westward tilted wave packet with a large vertical scale will further increase its vertical scale, whereas a westward-tilted wave packet with a small vertical scale further shrinks its vertical scale. This will have two important consequences for the forced oceanic responses. First, this effect will make the perturbation with a small vertical scale increase its vertical spatial scale and thus greatly strengthen the barotropic-like ocean response. At the same time it pushes the perturbations with a small vertical scale into further smaller scale. Thus this mechanism may separate the ocean responses into two extremes with different vertical scales. Second, since the zonal propagation speed increases with the vertical spatial scale of a westward tilted wave packet, the structure change will further increase the speed westward, reenforcing higher speeds in the western basin than in the eastern basin. These may also be relevant to the fact that the TOPEX/Poseidon observations show such a dominant counter-Doppler-shift mode in the sea-surface height anomalies in all major oceans and that the dominance increases westward.

d. Wave packet method

Mathematically the wave packet method could be still valid even when the local wave number approaches zero, but not at zero [e.g., Yang 1991). Using Lagrangian manifold formalism, one can easily show that the governing equations for the wave packet are valid even at caustics, (Gorman and Yang 2000). Even though the sea surface height anomalies observed in the TOPEX/Poseidon data extend several hundred kilometers in the zonal direction, the ocean basin is several thousands kilometers wide from coast to coast. Thus, the wave packet approximation is always valid in the zonal direction. However, in the vertical direction, the ocean depth is about 4000 to 5000 m. If the ocean response is concentrated within the thermocline, this assumption should be always valid. The assumption that the perturbation system varies slowly in the vertical may break down when the vertical scale of the ocean response becomes larger than that of the zonal flow. Unfortunately, the TOPEX/Poseidon data only provides the information on the horizontal scale at the sea surface. Thus, one really does not know exactly what the vertical scale of the perturbation system is that contributes to the observed sea surface height anomalies in the real oceans. Mathematically one always could change the relative vertical scale to make the analysis valid, for example, by requiring a local vertical wavenumber larger than the vertical mode number of the zonal basic flow.

Alternatively all other studies have used a layered model or normal mode with fixed vertical scale and vertical structure for the perturbation system. Those approaches thus avoid this problem in analysis. However, they cannot adequately describe the real evolution of the long planetary waves in the ocean. As discussed above, these vertical-scale changes, in fact, can be manifest in the observed TOPEX/Poseidon data.

Thus, like with any analytic approach, one should always take great care when applied our results to the real oceans. With the same token, one should take equal care when one interprets the data with any theory since the data represent an end result that may be caused by many factors and their interactions.

6. Main conclusions

In this study we investigate the evolution of a long planetary wave packet in baroclinic zonal currents in a

continuously stratified ocean in response to various forcing functions. From the above discussions we can draw the following main conclusions.

1) The evolution of a long planetary wave packet with a large vertical scale in a zonal current in response to atmospheric wind forcing at the sea surface and ocean topographic forcing on the sea floor, but not surface cooling or heating, may explain qualitatively all major features of the recently observed long planetary wave speeds in the TOPEX/Poseidon data, including enhanced (weakened) propagation speeds in the extratropics (Tropics) and in a western (eastern) basin, as well as an increase in the speed ratio with latitude.
2) For a wave packet with large vertical scale, effects of the stratification variation and vertical mode of mean zonal current make the wave packet propagate directly against the mean zonal current, the so-called counter-Doppler-shift effect. Dewar (1998) also noted this phenomenon. The effect of exponential variation on the wave speed may exactly cancel the advection effect, resulting in the non-Doppler-shift effect.
3) The β and stratification effects increase the vertical spatial scale of a vertically westward tilted wave packet and decrease the vertical scale of an eastward tilted wave packet.
4) The vertical scale of a wave packet plays an important role in the packet's structural change. For a wave packet with vertical scale larger (smaller) than the vertical mode scale of the mean current, the vertical spatial scale increases (decreases) when the wave packet is tilted westward in an eastward mean zonal current.
5) The vertical structural change in the wave packet may separate different ocean responses and strengthen the counter-Doppler-shift effect, resulting in an enhanced speed in the western ocean basin.

Even though present theory successfully predicts all major features of the TOPEX/Poseidon observations qualitatively, more detailed comparison could not be done due to the limitations of our model. In real oceans, the dominant ocean circulation is not zonal. Thus in a following study we extend our study by including a gyre ocean circulation (Yang 2000, manuscript submitted to *J. Phys. Oceanogr.*). It is found that the many features of the evolution of a wave packet still hold there. Therefore, future work should be focused on applying the theory to a real ocean circulation by using observed ocean current data and direct numerical modeling.

Acknowledgments. I would like to thank Drs. Z. Liu, R. X. Huang, J. Pedlosky, G. Mitchum, and W. Dewar for valuable discussions on the subject and Ms. J. Virmani for editorial assistance. The work was partially supported by the Research and Creative Scholarship Award of the USF Research Council.

APPENDIX

Other Wave Packet Solutions

a. Large vertical-scale wave packets

We assume that the wave packet is on the f plane, so $\beta = 0$, and the vertical scale of the wave packet is large; that is, $k^2\pi^2 \gg l^2$.

The governing system becomes

$$\frac{dm}{dT} = 0 \tag{A.1}$$

$$\frac{\epsilon dl}{dT} = \frac{2mHUk^2\pi^2}{1 + 4H^2l^2}[1 - 2Hk\pi \tan(k\pi z)] \tag{A.2}$$

$$\frac{dX}{dT} = -\frac{4H^2k^2\pi^2U}{1 + 4H^2l^2} \tag{A.3}$$

$$\frac{dZ}{dT} = \frac{8H^2mlU(1 + 4H^2k^2\pi^2)}{(1 + 4H^2l^2)^2}. \tag{A.4}$$

From (A.2) and (A.4) we have

$$\frac{dl}{dz} = \frac{k^2\pi^2(1 + 4H^2l^2)}{4lH(1 + 4H^2k^2\pi^2)}U[1 - 2Hk\pi \tan(k\pi z)]. \tag{A.5}$$

The solutions are given by

$$1 + 4H^2l^2 = (1 + 4H^2l_s^2)e^{pz/(2H)}[\cos(k\pi z)]^p, \tag{A.6}$$

where

$$p = \frac{4H^2k^2\pi^2}{1 + 4H^2k^2\pi^2}. \tag{A.7}$$

For $k = 1$ $p = 0.74$ and for $k = 2$, 3, and 4 $p = 0.92$, 0.96, and 0.98, respectively. Figure A1 shows the wave packet evolution in the (l, z) phase space for different vertical modes of the mean current. In the upper ocean, the vertical spatial scale of the wave packet increases (decreases) in the eastward mean current for an eastward (westward) tilted packet. The vertical scale decreases (increases) in the westward mean current for an eastward (westward) tilted packet. The middle of the ocean is of great interest, where a wave packet may oscillate vertically as it propagates.

b. Zero vertical mode

We consider a wave packet on the f plane with a zero vertical mode in the mean current. In this case, $k = \beta = 0$ and the system governing the evolution of the wave packet becomes

$$\frac{dm}{dT} = 0 \tag{A.8}$$

$$\frac{dl}{dT} = -\frac{2Hl^2mU}{1 + 4H^2l^2} \tag{A.9}$$

$$\frac{dX}{dT} = \frac{4H^2l^2U}{1 + 4H^2l^2} \tag{A.10}$$

$$\frac{dZ}{dT} = \frac{8H^2mlU}{(1 + 4H^2l^2)^2}. \tag{A.11}$$

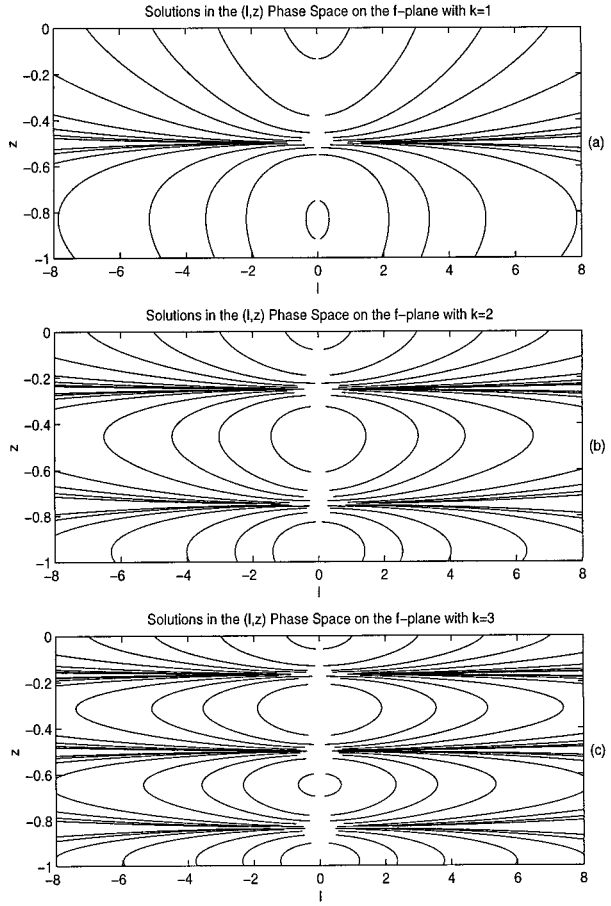

FIG. A1. Wave packet solutions in (l, z) phase space when the vertical scale of a wave packet is much larger than the vertical mode scale of the mean zonal current, that is, ($l^2 \ll k^2\pi^2$): (a) $k = 1$, (b) $k = 2$, and (c) $k = 3$.

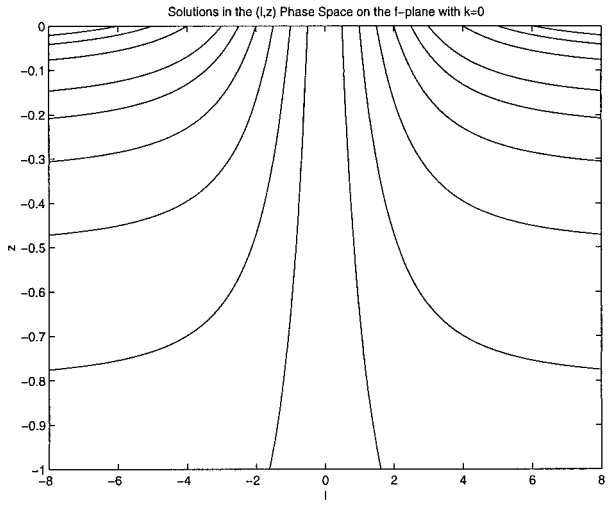

FIG. A2. Wave packet solutions in (l, z) phase space for the case where $k = \beta = 0$.

We can easily obtain the solution in the phase space (l, z):

$$4H^2 + l^{-2} = (4H^2 + l_s^{-2})e^{z/(2H)}. \quad \text{(A.12)}$$

Figure A2 shows the solution in the (l, z) phase space. It shows that for a westward tilted packet, the wave packet travels upward and its vertical spatial scale increases. For an eastward tilted packet, the wave packet travels downward and its vertical spatial scale decreases. Again, even though the vertical spatial scale of the packet changes with time, its zonal wave speed is constant. One can obtain the complete explicit solution

$$m = m_s \quad \text{(A.13)}$$

$$l = \pm 1/\sqrt{(4H^2 + l_s^{-2})e^{z/(2H)} - 4H^2} \quad \text{(A.14)}$$

$$X = X_s + \frac{4H^2U_s}{4H^2 + l_s^{-2}}(t - t_s) \quad \text{(A.15)}$$

$$z = 2H \ln\left\{\frac{4H^2}{4H^2 + l_s^{-2}} + \frac{4H^2 + l_s^{-2}}{[4HmU_s(t - t_s) + 4H^2 l_s + l_s^{-1}]^2}\right\}. \quad \text{(A.16)}$$

REFERENCES

Chelton, D. B., and M. G. Schlax, 1996: Global observations of oceanic Rossby waves. *Science*, **272,** 234–238.

Courant, R., and D. Hilbert, 1962: *Methods of Mathematical Physics.* Vol. II. John Wiley, 830 pp.

Dewar, W. K., 1998: On too ''fast'' baroclinic planetary waves in the general circulation. *J. Phys. Oceanogr.*, **28,** 1739–1758.

Dickson, R. E., 1978: Rossby waves—Long-period oscillations of oceans and atmospheres. *Annu. Rev. Fluid Mech.*, **10,** 159–195.

Gill, A. E., 1982: *Atmosphere–Ocean Dynamics.* Academic Press, 662 pp.

——, J. S. A. Green, and A. J. Simmons, 1974: Energy partition in the large-scale ocean circulation and the production of mid-ocean eddies. *Deep-Sea Res.*, **21,** 499–528.

Gorman, A., and H. Yang, 2000: Caustic consideration of the long planetary wave packet analysis in the continuously stratified ocean. *Int. J. Math. Math. Sci.*, in press.

Huang, R. X., and J. Pedlosky, 1999: Climate variability inferred from a layered model of the ventilated thermocline. *J. Phys. Oceanogr.*, **29,** 779–790.

Jacobs, G. A., W. J. Emery, and G. H. Born, 1993: Rossby waves in the Pacific Ocean extracted from Geosat altimeter data. *J. Phys. Oceanogr.*, **23,** 1155–1175.

——, H. E. Hurburt, J. C. Kindle, E. J. Metzger, J. L. Mitchell, W. J. Teague, and A. J. Wallcraft, 1994: Decade-scale trans-Pacific propagation and warming effects of an El Niño anomaly. *Nature*, **370,** 360–363.

Kang, Y. Q., and L. Magaard, 1980: Annual baroclinic Rossby waves in the central North Pacific. *J. Phys. Oceanogr.*, **10,** 1159–1167.

Kessler, W. S., 1990: Observations of long Rossby waves in the northern tropical Pacific. *J. Geophys. Res.*, **95,** 5183–5217.

Killworth, P. D., D. B. Chelton, and R. A. de Szoeke, 1997: The speed of observed and theoretical long extratropic planetary waves. *J. Phys. Oceanogr.*, **27,** 1946–1966.

Levitus, S., and T. Boyer, 1994: *World Ocean Atlas 1994.* Vol. 4, *Temperature*, NOAA Atlas NESDIS 4, U.S. Govt. Printing Office, 117 pp.

——, R. Burgett, and T. Boyer, 1994: *World Ocean Atlas 1994.* Vol.

3, *Salinity*, NOAA Atlas NESDIS 3, U.S. Govt. Printing Office, 99 pp.
Liu, Z., 1999: Forced planetary wave response in a thermocline gyre. *J. Phys. Oceanogr.*, **29,** 1036–1055.
Pedlosky, J., 1987: *Geophysical Fluid Dynamics.* Springer-Verlag, 710 pp.
Pillips, N. A., 1965: Elementary Rossby waves. *Tellus*, **17,** 295–301.
Platzman, G. W., 1968: The Rossby wave. *Quart. J. Roy. Meteor. Soc.*, **94,** 225–248.
Polito, P. S., and P. Cornillon, 1997: Long baroclinic Rossby waves detected by TOPEX/POSEIDON. *J. Geophys. Res.*, **102,** 3215–3235.
Schneider, N., A. J. Miller, M. A. Alexander, and C. Deser, 1999: Subduction of decadal North Pacific temperature anomalies: Observations and dynamics. *J. Phys. Oceanogr.*, **29,** 1056–1070.
White, W., 1977: Observations of long Rossby waves in the northern tropical Pacific. *J. Phys. Oceanogr.*, **7,** 50–61.
——, 1985: The resonant response of interannual baroclinic Rossby waves to wind forcing in the eastern midlatitude North Pacific. *J. Phys. Oceanogr.*, **15,** 403–415.
Yang, H., 1987: Evolution of a Rossby wave packet in barotropic flows with asymmetric basic current, topography and δ-effect. *J. Atmos. Sci.*, **44,** 2268–2276.
——, 1991: *Wave Packets and their Bifurcations in Geophysical Fluid Dynamics.* Applied Mathematical Sciences, Vol. 85, Springer-Verlag, 247 pp.